

Nonlinear-Gain Distributed Zeroth-Order Optimization for Networked Black-Box Control Extended Version

Shengjun Zhang, Tingyi Liu, Heng Zhang, and Dong Xie

Abstract—This letter studies distributed stochastic optimization over a peer-to-peer network when agents can query only zeroth-order function values. We propose ZOOM-PB, a coordinate-sampling distributed zeroth-order method equipped with a fractional-power powerball map. The proposed mechanism applies a nonlinear feedback gain directly to coordinate ZO estimates: it amplifies weak signals in flat regions and attenuates large stochastic estimates while transmitting only primal variables. Under standard smoothness, oracle-variance, and network-connectivity assumptions, ZOOM-PB achieves the leading nonconvex stationarity rate $\mathcal{O}(\sqrt{p/(nT)})$, where p is the decision dimension, n is the number of agents, and T is the iteration horizon. Under the Polyak–Łojasiewicz condition, it further attains the leading objective residual rate $\mathcal{O}(p/(nT))$. Thus the method preserves the known distributed ZO order while changing the finite-time behavior through a local nonlinear control gain. Simulations on black-box learning and sensor-driven UAV source seeking show faster empirical convergence in weak-signal regimes.

Index Terms—Distributed optimization, zeroth-order optimization, black-box control, multi-agent systems, powerball.

I. INTRODUCTION

Distributed optimization is a basic tool for networked control, machine learning, robotic swarms, and sensor networks, where agents cooperatively solve

$$\min_{x \in \mathbb{R}^p} f(x) \triangleq \frac{1}{n} \sum_{i=1}^n f_i(x), \quad f_i(x) = \mathbb{E}_{\xi_i} [F_i(x, \xi_i)]. \quad (1)$$

Many first-order distributed methods assume that each agent can compute or estimate $\nabla f_i(x)$ directly. This assumption is restrictive in black-box control and simulation-based optimization, where agents may observe only noisy function values, such as concentration readings in source seeking [1] or loss values in black-box learning [2]–[5].

Zeroth-order (ZO) methods replace gradients by finite-difference estimates and have been extensively studied in centralized stochastic optimization [6]–[9]. Distributed ZO methods further couple gradient estimation with network

consensus [10]–[16]. However, most existing distributed stochastic ZO algorithms follow one of two paths: they either use spherical perturbations with primal–dual or tracking variables, or they focus on asymptotic stationarity without addressing the transient slowdowns caused by small ZO signals in flat nonconvex regions. This issue arises naturally in black-box networked control, where agents may be far from an informative signal source and the finite-difference values are dominated by noise.

We introduce a nonlinear *powerball amplification* map into distributed ZO updates. For an estimated gradient component g , the map

$$\sigma(g, \gamma) = \text{sgn}(g)|g|^\gamma, \quad \gamma \in [1/2, 1], \quad (2)$$

is applied componentwise. When $|g| < 1$, it amplifies weak signals; when $|g| > 1$, it attenuates large estimates. Thus, from a control viewpoint, ZOOM-PB can be interpreted as a state-dependent nonlinear feedback gain rather than merely another finite-difference estimator. This is the main distinction from current distributed ZO methods. Powerball-type maps were originally studied for first-order descent methods [17]; here they are applied to noisy coordinate ZO estimates inside a peer-to-peer algorithm. The threshold $|g| = 1$ is relative to the normalization of the ZO estimate and can be absorbed into the stepsize scale.

With this mechanism, the paper makes three contributions. First, we propose a fully distributed stochastic ZO algorithm that exchanges only primal variables and uses coordinate-wise function queries, so different agents can explore different coordinate subspaces in parallel. Second, we prove the leading nonconvex stationarity rate $\mathcal{O}(\sqrt{p/(nT)})$ and the leading Polyak–Łojasiewicz (PL) objective rate $\mathcal{O}(p/(nT))$ under the same primal communication primitive, with the full finite-time bounds stated in Theorems 1–2. Third, we isolate the finite-time effect of the nonlinear powerball gain by comparing it with the linear endpoint $\gamma = 1$ in both black-box learning and sensor-driven UAV source seeking. The resulting distinction is mechanism-level: ZOOM-PB changes the local input applied to the distributed ZO recursion, while the oracle schedule and transmitted state remain unchanged.

The nonlinear map in (2) is not introduced as a heuristic stepsize change. For any nonzero component g ,

$$\frac{|\sigma(g, \gamma)|}{|g|} = |g|^{\gamma-1}. \quad (3)$$

Hence the feedback gain is larger than one in weak-signal regions $0 < |g| < 1$ and smaller than one for large estimates

This work was partially supported by the National Natural Science Foundation of China under grant 52307120 and the National Social Science Fund of China under grant 24CTJ010.

Shengjun Zhang is with the School of Artificial Intelligence, Hubei University, Wuhan, China. sj.zhang@hubu.edu.cn.

Tingyi Liu is with the School of Economics and Management, Wuhan University, Wuhan, China. 2019101050047@whu.edu.cn.

Heng Zhang is with the School of Electronic Information and Electrical Engineering, Shanghai Jiao Tong University, Shanghai, China. zhangheng_sjtu@sjtu.edu.cn.

Dong Xie is with Baidu Inc., Beijing, China. xiedong04@baidu.com.

$|g| > 1$. Existing distributed ZO schemes mainly change the estimator or add tracking variables; ZOOM-PB changes the local descent vector through this componentwise nonlinear gain while keeping the peer-to-peer communication primitive unchanged.

Proposition 1. *For any $\gamma \in (0, 1)$ and any scalar $g \neq 0$, the powerball map satisfies $|\sigma(g, \gamma)| > |g|$ if $|g| < 1$, $|\sigma(g, \gamma)| = |g|$ if $|g| = 1$, and $|\sigma(g, \gamma)| < |g|$ if $|g| > 1$. Moreover, $\sigma(g, \gamma)$ preserves the sign of g .*

Proof. The result follows directly from $|\sigma(g, \gamma)|/|g| = |g|^{\gamma-1}$ and $\gamma - 1 < 0$. Sign preservation follows from the definition of $\text{sgn}(\cdot)$. \square

Proposition 1 gives the control interpretation of ZOOM-PB. When agents operate far from an informative region, the estimated ZO signal is often small and stochastic; the fractional power increases the actuation magnitude without changing the descent direction. Near sharp regions or under large oracle perturbations, the same map attenuates the injected vector and helps avoid aggressive jumps. This effect does not change the asymptotic big- \mathcal{O} exponent, so the convergence-order claim and the nonlinear-gain claim are stated separately.

A. Relation to Existing Distributed ZO Methods

The proposed method should be distinguished from three nearby lines of work. The first line is centralized stochastic ZO optimization, where all function evaluations are collected by one processor or server. Such methods provide the baseline dimension dependence $\mathcal{O}(\sqrt{p/T})$ in nonconvex stochastic settings, but they do not exploit network parallelism and do not address peer-to-peer agreement. The rate in Theorem 1 replaces this term by $\mathcal{O}(\sqrt{p/(nT)})$ up to the consensus transient, which reflects the fact that n agents generate independent local ZO information.

The second line is deterministic distributed ZO optimization. These algorithms are valuable when each local cost can be queried exactly, but they do not model streaming stochastic function values. In networked sensing and black-box control, the local oracle often includes sampling noise, environmental disturbances, or minibatch randomness. The oracle model in Assumption 3 keeps this stochastic component explicit, and the Lyapunov recursion separates it from the topology-induced error.

The third and closest line is stochastic distributed ZO with primal-dual, tracking, or feedback-optimization mechanisms. ZOD-PDA and ZODIAC achieve linear speedup rates under stochastic nonconvex objectives, and the accelerated distributed ZO method in [18] also uses a powerball-type nonlinear gain within a primal-dual architecture. Multi-agent ZO feedback optimization studies gradient-free control loops with cooperative agents [16]. In contrast, ZOOM-PB keeps the communication state primal-only: agents send only their current decisions, local directions need not be coordinated across the network, and the nonlinear gain is applied locally to the coordinate-ZO estimate.

The analysis separates rate preservation from gain shaping. ZOOM-PB is not a claim of a new minimax exponent; it shows that a fractional-power ZO feedback gain can be inserted into a distributed stochastic coordinate-ZO recursion without losing the standard order. The simulations then test the finite-time regime in which the nonlinear input response is expected to matter.

II. PROBLEM SETUP AND ALGORITHM

Let $\mathcal{G} = (\mathcal{V}, \mathcal{E})$ be an undirected connected graph with Laplacian L . Define $\mathbf{L} = L \otimes I_p$, $K_n = I_n - \mathbf{1}\mathbf{1}^\top/n$, $\mathbf{K} = K_n \otimes I_p$, $\mathbf{H} = (\mathbf{1}\mathbf{1}^\top/n) \otimes I_p$, and $\bar{x}_k = \frac{1}{n} \sum_{i=1}^n x_{i,k}$. The agents minimize (1) using only evaluations of $F_i(\cdot, \xi_i)$.

Assumption 1. *The undirected graph \mathcal{G} is connected. The optimal set is nonempty, and the optimal value satisfies $f^* > -\infty$.*

Assumption 2. *For almost all ξ_i , the stochastic ZO oracle $F_i(\cdot, \xi_i)$ is L_f -smooth.*

Assumption 3. *For each coordinate j , $\mathbb{E}_{\xi_i}[(\nabla F_i(x, \xi_i) - \nabla f_i(x))^2] \leq \zeta^2$ for all i and x . Moreover, there exists σ_2 such that $\|\nabla f_i(x) - \nabla f(x)\|^2 \leq \sigma_2^2$ for all i and x . Conditioned on the history, the oracle samples $\xi_{i,k}$ and coordinate subsets $\mathcal{S}_{i,k}$ are independent across agents and iterations. Each $\mathcal{S}_{i,k}$ is sampled uniformly with cardinality n_c .*

Assumption 4. *Along the generated network-average sequence $\{\bar{x}_k\}$, there exists a deterministic constant $G \geq 1$ such that $\|\nabla f(\bar{x}_k)\|_\infty \leq G$ for all k almost surely.*

Assumption 4 is used only to convert the nonlinear descent term into a squared-gradient term through $\nabla f(\bar{x}_k)^\top \sigma(\nabla f(\bar{x}_k), \gamma) \geq G^{\gamma-1} \|\nabla f(\bar{x}_k)\|^2$. It is weaker than assuming uniformly bounded local gradients on the whole domain. It holds, for example, under compact level sets, projected implementations, or physically bounded search domains.

At iteration k , agent i samples a coordinate subset $\mathcal{S}_{i,k} \subseteq \{1, \dots, p\}$ with cardinality n_c and constructs either the one-point or two-point coordinate estimator

$$g_{i,k}^e = \frac{p}{n_c} \sum_{\ell \in \mathcal{S}_{i,k}} \frac{F_i(x_{i,k} + \delta_{\ell,k} e_\ell, \xi_i) - F_i(x_{i,k}, \xi_i)}{\delta_{\ell,k}} e_\ell, \quad (4)$$

$$g_{i,k}^e = \frac{p}{n_c} \sum_{\ell \in \mathcal{S}_{i,k}} \frac{F_i(x_{i,k} + \delta_{\ell,k} e_\ell, \xi_i)}{2\delta_{\ell,k}} e_\ell - \frac{p}{n_c} \sum_{\ell \in \mathcal{S}_{i,k}} \frac{F_i(x_{i,k} - \delta_{\ell,k} e_\ell, \xi_i)}{2\delta_{\ell,k}} e_\ell. \quad (5)$$

The coordinate form is useful in a network: the sampling burden associated with p can be distributed across agents instead of being concentrated in a single oracle. With n_c sampled coordinates, each iteration uses $n_c + 1$ function values for (4) or $2n_c$ function values for (5) per agent, and each agent broadcasts one p -dimensional primal vector to its neighbors. No dual variables, gradient trackers, or raw data samples are transmitted.

TABLE I
POSITIONING AGAINST REPRESENTATIVE ZERO-ORDER OPTIMIZATION METHODS

Method	Setting	Oracle/comm.	Rate or limitation
Centralized ZO [6], [7]	Stochastic	Server-based	$\mathcal{O}(\sqrt{p/T})$
ZO-GDA [12]	Deterministic	Spherical ZO, primal	Deterministic convergence
ZONE-M [13]	Stochastic	Multi-point ZO, primal/dual	$\mathcal{O}(p^2 n/T)$ with large sampling
Primal-dual accelerated ZO [14], [15], [18]	Stochastic	ZO, primal/dual	Linear-speedup rates; acceleration uses auxiliary states
ZOOM-PB	Stochastic	Coordinate ZO, primal only	$\mathcal{O}(\sqrt{p/(nT)})$; PL: $\mathcal{O}(p/(nT))$

Algorithm 1 ZOOM-PB

- 1: **Input:** $\alpha > 0$, $\gamma \in [1/2, 1]$, steps $\{\eta_k\}$, radii $\{\delta_{\ell,k}\}$.
- 2: **Initialize:** $x_{i,0} \in \mathbb{R}^p$ for all $i \in [n]$.
- 3: **for** $k = 0, 1, \dots$ **do**
- 4: **for** each agent i in parallel **do**
- 5: Exchange $x_{i,k}$ with neighbors $j \in \mathcal{N}_i$.
- 6: Form $g_{i,k}^e$ by (4) or (5).
- 7: Update

$$x_{i,k+1} = x_{i,k} - \alpha \sum_{j=1}^n L_{ij} x_{j,k} - \eta_k \sigma(g_{i,k}^e, \gamma).$$

- 8: **end for**
 - 9: **end for**
-

When $\gamma = 1$, Algorithm 1 reduces to the baseline ZOOM algorithm. Therefore, ZOOM is not treated as a separate method in this letter; it is the linear-gain endpoint of ZOOM-PB.

A. Algorithmic Distinction

The proposed update differs from existing distributed stochastic ZO methods along three dimensions. First, it is *coordinate-parallel*: each agent samples a small coordinate subset, and the network collectively explores the decision space. This is different from spherical smoothing, where each oracle call perturbs all coordinates and may suffer from larger high-dimensional variance. Second, it is *primal-only*: agents exchange $x_{i,k}$ but do not transmit dual variables, gradient trackers, or query directions. This lowers the communication state relative to primal–dual ZO schemes. Third, it is *nonlinearly amplified*: after the ZO estimate is constructed, the powerball map reshapes the descent vector componentwise. ZOOM-PB is therefore a distributed ZO controller with a state-dependent input nonlinearity.

For each iteration and each agent, the one-point coordinate estimator uses $n_c + 1$ function evaluations and the two-point estimator uses $2n_c$ function evaluations. The communication payload is one p -dimensional primal vector to neighboring agents. Thus the method adds no auxiliary communication state beyond the decision variable itself. The coordinate estimators may use more function values than a two-point spherical estimator when $n_c > 1$, but they avoid perturbing all coordinates at once and support agent-level parallelism. In black-box control applications where function queries are local sensor readings or simulator calls, this tradeoff can be

favorable because each agent obtains its own measurements independently.

Over a horizon of T iterations, the resulting network query budget is $nT(n_c + 1)$ for the one-point estimator and $2nTn_c$ for the two-point estimator. If each endpoint-to-neighbor transmission is counted as one directed message, the communication cost is $2|\mathcal{E}|Tp$ scalar transmissions, the same order as a primal consensus method. These budgets are independent of γ : the exponent changes only the local post-processing of $g_{i,k}^e$, not the oracle schedule, the graph messages, or the dimension of the communicated state. Hence the empirical differences reported below are due to gain shaping under the same communication primitive, not to extra samples or extra consensus variables.

III. CONVERGENCE RESULTS

The analysis tracks two coupled quantities: the consensus disagreement $\|\mathbf{x}_k\|_{\mathbf{K}}^2$ and the descent of the network average \bar{x}_k . Let $\mathbf{g}_k^e = \text{col}(g_{1,k}^e, \dots, g_{n,k}^e)$. Constants C , a_i , and c_i may depend on the problem and graph parameters, but not on T ; all displayed p - and n -dependences are explicit. Since $\mathbf{1}^\top L = 0$, the network average evolves as

$$\bar{x}_{k+1} = \bar{x}_k - \frac{\eta_k}{n} \sum_{i=1}^n \sigma(g_{i,k}^e, \gamma). \quad (6)$$

Thus, from the viewpoint of the averaged optimizer, the Laplacian term does not directly move \bar{x}_k ; it only controls how well the local queries are centered around the same point. The proof therefore tracks the optimization error and the consensus error together. The disagreement component satisfies the recursion

$$\mathbf{K}\mathbf{x}_{k+1} = \mathbf{K}(I_{np} - \alpha\mathbf{L})\mathbf{x}_k - \eta_k \mathbf{K}\sigma(\mathbf{g}_k^e, \gamma), \quad (7)$$

where the spectral gap of L contracts the first term, while the nonlinear ZO input creates a stochastic perturbation. Lemma 1 collects the estimates needed to balance these two effects.

Lemma 1. *Let \mathcal{F}_k be the history before the oracle calls at time k and set $\bar{s}_k = n^{-1} \sum_{i=1}^n \sigma(g_{i,k}^e, \gamma)$. Under Assump-*

tions 1–4, Algorithm 1 satisfies

$$\mathbb{E}[\|\bar{s}_k\|^2 \mid \mathcal{F}_k] \leq c_1 \|\nabla f(\bar{x}_k)\|^2 + c_2 \frac{\|\mathbf{x}_k\|_{\mathbf{K}}^2}{n} + c_3 \frac{p}{n} + c_4 \frac{p^2 \delta_k^2}{n}, \quad (8a)$$

$$\mathbb{E}[W_{k+1}] \leq W_k - \frac{c_5}{n} \|\mathbf{x}_k\|_{\mathbf{K}}^2 - c_6 n \eta_k \|\nabla f(\bar{x}_k)\|^2 + c_7 p \eta_k^2 + c_8 p^2 \eta_k \delta_k^2, \quad (8b)$$

where W_k is a nonnegative Lyapunov function equivalent to $n(f(\bar{x}_k) - f^*) + \|\mathbf{x}_k\|_{\mathbf{K}}^2/n$.

Proof. Condition on \mathcal{F}_k . For each agent, the coordinate estimator can be written as $g_{i,k}^e = \nabla f_i(x_{i,k}) + \varepsilon_{i,k} + b_{i,k}$, where $\mathbb{E}[\varepsilon_{i,k} \mid \mathcal{F}_k] = 0$, $\mathbb{E}[\|\varepsilon_{i,k}\|^2 \mid \mathcal{F}_k] \leq Cp$ after the usual coordinate-sampling scaling, and $\|b_{i,k}\| \leq Cp\delta_k$ is the finite-difference bias. Independence across agents gives the variance reduction

$$\mathbb{E} \left[\left\| \frac{1}{n} \sum_{i=1}^n \varepsilon_{i,k} \right\|^2 \mid \mathcal{F}_k \right] \leq C \frac{p}{n}.$$

Smoothness and gradient heterogeneity imply $n^{-1} \sum_i \|\nabla f_i(x_{i,k}) - \nabla f(\bar{x}_k)\|^2 \leq C \|\mathbf{x}_k\|_{\mathbf{K}}^2/n + C$. Since $\gamma \in [1/2, 1]$, the scalar inequality $|z|^{2\gamma} \leq 1 + z^2$ gives $\|\sigma(u, \gamma)\|^2 \leq C(1 + \|u\|^2)$. Combining these estimates yields the averaged moment bound (8a); after averaging over agents, the oracle-noise term scales as p/n rather than np .

For the Lyapunov step, take $W_{1,k} = \|\mathbf{x}_k\|_{\mathbf{K}}^2/(2n)$ and $W_{2,k} = n(f(\bar{x}_k) - f^*)$. The consensus update gives

$$\mathbb{E}[W_{1,k+1}] \leq W_{1,k} - a_1 \frac{\|\mathbf{x}_k\|_{\mathbf{K}}^2}{n} + a_2 \eta_k^2 \mathbb{E}[\|\bar{s}_k\|^2 \mid \mathcal{F}_k] + a_3 p^2 \eta_k \delta_k^2, \quad (9)$$

where $a_1 > 0$ follows from $\alpha < \rho_2(L)/(2\rho(L^2))$. For the averaged iterate, $\bar{x}_{k+1} = \bar{x}_k - \eta_k \bar{s}_k$, and smoothness gives

$$\mathbb{E}[W_{2,k+1}] \leq W_{2,k} - a_4 n \eta_k \|\nabla f(\bar{x}_k)\|^2 + a_5 \eta_k \|\mathbf{x}_k\|_{\mathbf{K}}^2 + a_6 p \eta_k^2 + a_7 p^2 \eta_k \delta_k^2. \quad (10)$$

Here the descent coefficient uses Assumption 4: for $u = \nabla f(\bar{x}_k)$, $\nabla f(\bar{x}_k)^\top \sigma(\nabla f(\bar{x}_k), \gamma) = \sum_j |\nabla_j f(\bar{x}_k)|^{1+\gamma} \geq G^{\gamma-1} \|\nabla f(\bar{x}_k)\|^2$. Choosing t_1 or a constant upper bound on η_k small enough, the $a_5 \eta_k \|\mathbf{x}_k\|_{\mathbf{K}}^2$ term is absorbed by the consensus contraction. Substituting (8a) and collecting constants gives (8b). \square

Theorem 1. *Suppose Assumptions 1–4 hold. Let $\{\mathbf{x}_k\}$ be generated by Algorithm 1. For any $T \geq n^3/p$, choose*

$$\alpha \in \left(0, \frac{\rho_2(L)}{2\rho(L^2)}\right), \quad \eta_k = \frac{\sqrt{n}}{\sqrt{pT}}, \quad \delta_{i,k} \leq \frac{\kappa_\delta}{p^{1/4} n^{1/4} (k+1)^{1/4}}. \quad (11)$$

Then

$$\frac{1}{T} \sum_{k=0}^{T-1} \mathbb{E}[\|\nabla f(\bar{x}_k)\|^2] = \mathcal{O}\left(\sqrt{\frac{p}{nT}}\right) + \mathcal{O}\left(\frac{n}{T}\right), \quad (12a)$$

$$\frac{1}{T} \sum_{k=0}^{T-1} \mathbb{E}\left[\frac{1}{n} \sum_{i=1}^n \|x_{i,k} - \bar{x}_k\|^2\right] = \mathcal{O}\left(\frac{n}{T}\right). \quad (12b)$$

Proof. Summing (8b) from 0 to $T-1$ and using $W_T \geq 0$ give

$$\frac{c_5}{n} \sum_{k=0}^{T-1} \mathbb{E}[\|\mathbf{x}_k\|_{\mathbf{K}}^2] + c_6 n \eta \sum_{k=0}^{T-1} \mathbb{E}[\|\nabla f(\bar{x}_k)\|^2] \leq W_0 + c_7 p T \eta^2 + c_8 p^2 \eta \sum_{k=0}^{T-1} \delta_k^2. \quad (13)$$

With $\eta = \sqrt{n/(pT)}$, the averaged oracle term satisfies $pT\eta^2/(nT\eta) = \sqrt{p/(nT)}$. Dividing (13) by $nT\eta$ therefore yields the stationarity estimate, while the initial condition and consensus transient give the displayed $\mathcal{O}(n/T)$ term under $T \geq n^3/p$. The smoothing schedule makes the finite-difference bias lower order after constants are collected. Dividing (13) by T and using the first term on the left gives the averaged disagreement bound. \square

The two terms in Theorem 1 have different origins. The term $\mathcal{O}(\sqrt{p/(nT)})$ is the statistical ZO term: the dimension p appears because finite-difference estimation is harder in high dimension, while the factor n appears because the network performs n independent local queries per iteration. The term $\mathcal{O}(n/T)$ is a transient network term caused by imperfect agreement among agents. For long horizons, or for moderately connected graphs, this transient is dominated by the stochastic ZO term. This interpretation is useful for choosing the network size: adding agents improves the statistical term but also increases the consensus transient, so the topology and time horizon should be matched.

Assumption 5. *The global function f satisfies the PL condition with constant $\nu > 0$, i.e., $\frac{1}{2} \|\nabla f(x)\|^2 \geq \nu(f(x) - f^*)$ for all x .*

Theorem 2. *Suppose Assumptions 1–5 hold and ν is known. Let*

$$\eta_k = \frac{\kappa_\eta}{k+t_1}, \quad \delta_{i,k} \leq \frac{\kappa_\delta \sqrt{p\eta_k}}{\sqrt{n+p}}, \quad (14)$$

where $\kappa_\eta > 8/\nu$ and t_1 is large enough so that the requirements of Lemma 1 hold for all k . Then, for all $T \geq 1$,

$$\mathbb{E}\left[\frac{1}{n} \sum_{i=1}^n \|x_{i,T} - \bar{x}_T\|^2\right] = \mathcal{O}\left(\frac{p}{T^2}\right), \quad (15a)$$

$$\mathbb{E}[f(\bar{x}_T) - f^*] = \mathcal{O}\left(\frac{p}{nT}\right) + \mathcal{O}\left(\frac{p}{T^2}\right). \quad (15b)$$

Proof. Under the PL condition, $n \|\nabla f(\bar{x}_k)\|^2 \geq 2\nu n(f(\bar{x}_k) - f^*)$. Substituting this into (8b) and using the definition of W_k yields

$$\mathbb{E}[W_{k+1}] \leq (1 - c\eta_k)W_k + \mathcal{O}(p\eta_k^2).$$

With $\eta_k = \kappa_\eta / (k + t_1)$ and $\kappa_\eta > 8/\nu$, a standard diminishing-step sequence lemma gives

$$\mathbb{E}[W_T] = \mathcal{O}\left(\frac{p}{T}\right). \quad (16)$$

Applying the disagreement part of (8b) once more with the already bounded objective term yields

$$\mathbb{E}\left[\frac{\|\mathbf{x}_T\|_{\mathbf{K}}^2}{n}\right] = \mathcal{O}\left(\frac{p}{T^2}\right). \quad (17)$$

Finally, since W_T is equivalent to $\|\mathbf{x}_T\|_{\mathbf{K}}^2 / n + n(f(\bar{x}_T) - f^*)$, division by n gives the objective residual bound. \square

The PL result should not be read as a convexity result. It applies to a class of nonconvex objectives where every stationary point is globally optimal, which is common in several over-parameterized or structured estimation problems. The sharper $\mathcal{O}(p/(nT))$ term shows that, once the gradient norm controls the objective residual, the same network-level sampling effect provides linear speedup in the optimization error itself.

Remark 1. *Theorems 1–2 show that the nonlinear gain does not change the leading p, n, T order under the stated conditions. The gain is instead used to alter the finite-time input response of the coordinate-ZO recursion while retaining primal-only communication.*

Proposition 2. *All conclusions of Theorems 1 and 2 also hold for ZOOM, obtained by setting $\gamma = 1$ in Algorithm 1. In this case, $\sigma(g, 1) = g$, so the update is the linear-gain endpoint of the same coordinate-ZO recursion.*

Proof. When $\gamma = 1$, the nonlinear map reduces to the identity. The moment bound in Lemma 1 then specializes to the standard second-moment bound for the coordinate ZO estimator, and the Lyapunov recursion remains valid with the same averaged-oracle variance reduction. The two theorem statements follow without changing the step-size schedules. \square

This endpoint serves as the experimental control: comparing $\gamma < 1$ with $\gamma = 1$ isolates the nonlinear amplification from coordinate sampling and distributed consensus.

A. Parameter Choice

The parameter γ controls the strength of nonlinear amplification. Smaller values produce a stronger boost for weak components but also increase the sensitivity of the update near zero. In the theoretical analysis, $\gamma \in [1/2, 1]$ is used to control the powerball moment and descent terms in Lemma 1. In practice, values in $[0.5, 0.9]$ work robustly in our tests, with $\gamma = 0.7$ used as the default unless otherwise stated. The smoothing radius $\delta_{i,k}$ follows the theorem schedules and is decreased over time to reduce finite-difference bias.

IV. NUMERICAL EXAMPLES

A. Black-Box Binary Classification

We first use the nonlinear least-squares benchmark in [9]. The local loss is $f_i(x) = (y_i - \phi(x; a_i))^2$ with $\phi(x; a_i) = 1/(1 + \exp(-a_i^\top x))$. The training and test sets contain 2000 and 200 samples, respectively, $p = 100$, $n = 10$, and the communication graph follows the Erdős–Rényi model with connection probability 0.4. ZOOM-PB is compared with ZO-GDA [12], ZONE-M [13], ZOD-PDA [14], and ZODIAC [15]. Fig. 1 reports the training-loss curves.

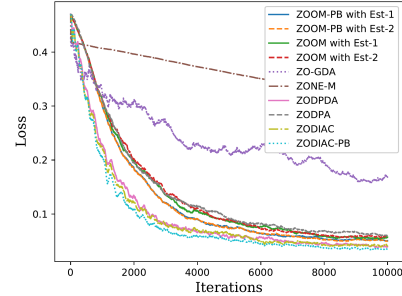


Fig. 1. Training-loss comparison on the black-box binary classification benchmark. ZOOM-PB accelerates the primal-only ZOOM endpoint while retaining comparable final test accuracy.

The direct ablation in Fig. 1 is ZOOM-PB versus the linear endpoint ZOOM, since both use the same coordinate-sampling oracle and exchange the same primal vector. The lower training loss of ZOOM-PB is therefore attributable to the nonlinear gain rather than to tracking dynamics or a different estimator. The final test accuracies remain close across the strongest methods: ZOOM-PB reaches 97.0%, ZOOM reaches 96.5%, and ZODIAC reaches 97.0%.

B. UAV Source Seeking

To emphasize the networked-control motivation, we consider a UAV swarm that searches for a hazardous emission source using only local concentration measurements. This is a black-box control task: each UAV observes a scalar sensor value at its current position and communicates only the current source estimate with neighboring UAVs. No concentration gradient, global field map, or centralized coordinator is used. The field is a nonconvex Gaussian mixture

$$\mathcal{H}(\xi) = \sum_{j=1}^3 A_j \exp\left(-\frac{\|\xi - c_j\|^2}{2\sigma_j^2}\right), \quad (18)$$

with the primary source at $c_1 = [5, 5]^\top$ and two weaker interference peaks. Let $p_i \in \mathbb{R}^2$ denote the physical position of UAV i . Its noisy measurement is $y_i = \mathcal{H}(p_i) + \omega_i$, where ω_i is sensor noise. Given the prior decay profile of the primary source, agent i minimizes

$$f_i(x) = \frac{1}{2} \left(y_i - A_1 \exp\left(-\frac{\|x - p_i\|^2}{2\sigma_1^2}\right) \right)^2. \quad (19)$$

The decision variable x is the estimated source location. The exponential observation model produces broad flat regions when the swarm is far from the source, making this task a natural test for nonlinear ZO amplification. Figs. 2–3 show the local source-estimate trajectories and compare the concentration response with the linear endpoint under the same oracle and communication budget.

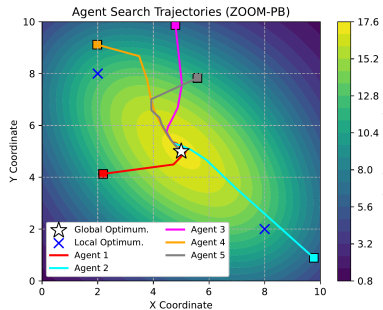


Fig. 2. Source-estimate trajectories under ZOOM-PB. Agents use only local concentration measurements and neighbor communication while moving their local estimates toward the primary peak.

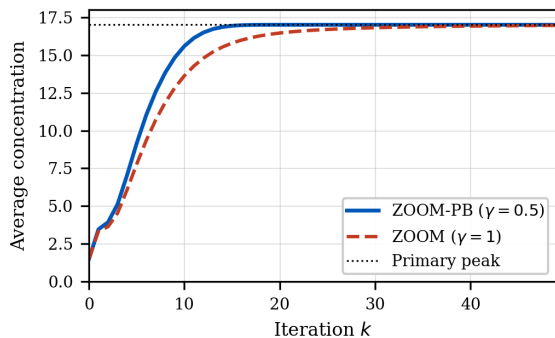


Fig. 3. Network-wide average concentration in the UAV source-seeking task. ZOOM-PB is compared with the linear endpoint ZOOM under the same coordinate-query and primal-communication budget.

This example reflects the intended networked-control setting: the objective is induced by sensor readings, the query oracle is local to each agent, and the useful search direction can be weak far away from the source. The paths in Fig. 2 are local source estimates; the physical UAV positions enter through the sensing model. In Fig. 3, the comparison between ZOOM-PB and ZOOM isolates the effect of replacing the linear gain by the fractional-power gain. The faster rise of the concentration curve is consistent with the gain acting mainly during the low-signal phase, before both methods approach the same source region. This improvement is obtained without adding tracking states, dual variables, or centralized coordination.

V. CONCLUSION

This letter proposed ZOOM-PB, a powerball-amplified distributed stochastic ZO method for black-box networked optimization. The method applies a componentwise nonlinear

feedback gain to coordinate ZO estimates while retaining primal-only communication. The analysis shows that this local nonlinear input preserves the standard distributed stochastic ZO rate, and the PL result gives a sharper objective residual under the same communication primitive. The simulations show faster transient behavior in black-box learning and sensor-driven UAV source seeking, especially when the useful ZO signal is small. Future work will study event-triggered or compressed communication variants, where the nonlinear ZO gain and communication noise interact.

VI. APPENDIX A: AUXILIARY ESTIMATOR BOUNDS

This appendix gives the technical details that are compressed in the main text. The constants below may change from line to line. They may depend on $L_f, \zeta, \sigma_2, n_c, \gamma, G$ and on fixed graph constants, but not on T, p , or n unless those dependences are displayed.

Let \mathcal{F}_k be the sigma-field generated by all iterates and oracle samples before the function queries at time k . For either coordinate estimator in (4)–(5), define the local error decomposition

$$g_{i,k}^e = \nabla f_i(x_{i,k}) + \varepsilon_{i,k} + b_{i,k}. \quad (20)$$

The term $\varepsilon_{i,k}$ contains coordinate-sampling and oracle noise, and $b_{i,k}$ contains finite-difference bias. By uniform coordinate sampling, oracle independence, and Assumption 3,

$$\mathbb{E}[\varepsilon_{i,k} \mid \mathcal{F}_k] = 0, \quad (21)$$

$$\mathbb{E}[\|\varepsilon_{i,k}\|^2 \mid \mathcal{F}_k] \leq Cp, \quad (22)$$

$$\|b_{i,k}\| \leq Cp\delta_k. \quad (23)$$

For the one-point estimator the last bound follows from smoothness of $F_i(\cdot, \xi_i)$ and the forward finite-difference remainder. For the two-point estimator, the same order is retained under the common first-order smoothness assumption used in the letter; with a second-order smooth oracle this bias term can be sharpened, but the stated schedules do not require that sharpening.

The network average benefits from agent-level independence. Specifically,

$$\begin{aligned} \mathbb{E} \left[\left\| \frac{1}{n} \sum_{i=1}^n \varepsilon_{i,k} \right\|^2 \mid \mathcal{F}_k \right] &= \frac{1}{n^2} \sum_{i=1}^n \mathbb{E}[\|\varepsilon_{i,k}\|^2 \mid \mathcal{F}_k] \\ &\leq C \frac{p}{n}. \end{aligned} \quad (24)$$

The local-gradient mismatch satisfies the following bound. Denote

$$\begin{aligned} D_k &= \frac{1}{n} \sum_{i=1}^n \|\nabla f_i(x_{i,k}) - \nabla f(\bar{x}_k)\|^2. \\ D_k &\leq \frac{2}{n} \sum_{i=1}^n \|\nabla f_i(x_{i,k}) - \nabla f_i(\bar{x}_k)\|^2 \\ &\quad + \frac{2}{n} \sum_{i=1}^n \|\nabla f_i(\bar{x}_k) - \nabla f(\bar{x}_k)\|^2 \\ &\leq C \frac{\|\mathbf{x}_k\|_K^2}{n} + C\sigma_2^2. \end{aligned} \quad (25)$$

For $\gamma \in [1/2, 1]$, the scalar inequality $|z|^{2\gamma} \leq 1 + z^2$ and the monotonicity of $z \mapsto \text{sign}(z)|z|^\gamma$ give

$$\|\sigma(u, \gamma)\|^2 \leq C(1 + \|u\|^2), \quad (26)$$

$$(u - v)^\top (\sigma(u, \gamma) - \sigma(v, \gamma)) \geq 0. \quad (27)$$

Combining this bound with (24)–(25) gives the averaged nonlinear-oracle estimate

$$\begin{aligned} \mathbb{E}[\|\bar{s}_k\|^2 \mid \mathcal{F}_k] &\leq C \|\nabla f(\bar{x}_k)\|^2 + C \frac{\|\mathbf{x}_k\|_{\mathbf{K}}^2}{n} \\ &\quad + C \frac{p}{n} + C \frac{p^2 \delta_k^2}{n}, \end{aligned} \quad (28)$$

which is the detailed form of (8a). After averaging over agents, the random oracle term scales as p/n .

VII. APPENDIX B: DETAILED PROOF OF LEMMA 1

Let

$$\begin{aligned} W_{1,k} &= \frac{1}{2n} \|\mathbf{x}_k\|_{\mathbf{K}}^2, \\ W_{2,k} &= n(f(\bar{x}_k) - f^*), \\ W_k &= W_{1,k} + \lambda W_{2,k}, \end{aligned}$$

where $\lambda > 0$ is fixed below. Since $K_n L = L K_n = L$ and $K_n \mathbf{1} = 0$, the disagreement recursion is

$$\mathbf{K} \mathbf{x}_{k+1} = \mathbf{K}(I_{np} - \alpha \mathbf{L}) \mathbf{x}_k - \eta_k \mathbf{K} \sigma(\mathbf{g}_k^e, \gamma). \quad (29)$$

For $\alpha < \rho_2(L)/(2\rho(L^2))$, the consensus matrix is contractive on the disagreement subspace, so

$$\|\mathbf{K}(I_{np} - \alpha \mathbf{L}) \mathbf{x}_k\|^2 \leq (1 - \mu_L) \|\mathbf{x}_k\|_{\mathbf{K}}^2 \quad (30)$$

for some $\mu_L > 0$. Using Young's inequality and the averaged moment bound gives

$$\begin{aligned} \mathbb{E}[W_{1,k+1} \mid \mathcal{F}_k] &\leq W_{1,k} - c_L \frac{\|\mathbf{x}_k\|_{\mathbf{K}}^2}{n} + C \eta_k^2 \mathbb{E}[\|\bar{s}_k\|^2 \mid \mathcal{F}_k] \\ &\quad + C p^2 \eta_k \delta_k^2. \end{aligned} \quad (31)$$

The last bias term comes from the deterministic finite-difference remainder.

For the averaged iterate, since $\bar{x}_{k+1} = \bar{x}_k - \eta_k \bar{s}_k$, smoothness of f yields

$$\begin{aligned} \mathbb{E}[f(\bar{x}_{k+1}) \mid \mathcal{F}_k] &\leq f(\bar{x}_k) - \eta_k \nabla f(\bar{x}_k)^\top \mathbb{E}[\bar{s}_k \mid \mathcal{F}_k] \\ &\quad + \frac{L_f \eta_k^2}{2} \mathbb{E}[\|\bar{s}_k\|^2 \mid \mathcal{F}_k]. \end{aligned} \quad (32)$$

The first-order part of $\mathbb{E}[\bar{s}_k \mid \mathcal{F}_k]$ is $n^{-1} \sum_i \sigma(\nabla f_i(x_{i,k}), \gamma)$ up to finite-difference bias. Using monotonicity of the componentwise powerball map and the local-gradient mismatch bound, and denoting the left-hand side below by Φ_k ,

$$\begin{aligned} \Phi_k &\geq c_\gamma \|\nabla f(\bar{x}_k)\|^2 - C \frac{\|\mathbf{x}_k\|_{\mathbf{K}}^2}{n} \\ &\quad - C p^2 \delta_k^2, \end{aligned} \quad (33)$$

where $c_\gamma = G^{\gamma-1}$ follows from Assumption 4 applied to $u = \nabla f(\bar{x}_k)$, since $u^\top \sigma(u, \gamma) = \sum_j |u_j|^{1+\gamma} \geq G^{\gamma-1} \|u\|^2$

whenever $\|u\|_\infty \leq G$. Substituting this relation into (32) and multiplying by n gives

$$\begin{aligned} \mathbb{E}[W_{2,k+1} \mid \mathcal{F}_k] &\leq W_{2,k} - c_\gamma n \eta_k \|\nabla f(\bar{x}_k)\|^2 + C \eta_k \|\mathbf{x}_k\|_{\mathbf{K}}^2 \\ &\quad + C p \eta_k^2 + C p^2 \eta_k \delta_k^2. \end{aligned} \quad (34)$$

Combining (31) and (34), choosing λ and then the upper bound on η_k so that the positive $\eta_k \|\mathbf{x}_k\|_{\mathbf{K}}^2$ term is absorbed by the consensus contraction, and taking total expectations yields (8b).

VIII. APPENDIX C: DETAILED PROOF OF THEOREM 1

Summing (8b) gives

$$\begin{aligned} \frac{c_5}{n} \sum_{k=0}^{T-1} \mathbb{E}[\|\mathbf{x}_k\|_{\mathbf{K}}^2] + c_6 n \eta \sum_{k=0}^{T-1} \mathbb{E}[\|\nabla f(\bar{x}_k)\|^2] \\ \leq W_0 + C p T \eta^2 + C p^2 \eta \sum_{k=0}^{T-1} \delta_k^2. \end{aligned} \quad (35)$$

With $\eta = \sqrt{n/(pT)}$,

$$\frac{pT\eta^2}{nT\eta} = \sqrt{\frac{p}{nT}}.$$

The finite-difference schedule gives

$$\sum_{k=0}^{T-1} \delta_k^2 \leq C \frac{T^{1/2}}{p^{1/2} n^{1/2}},$$

so the smoothing-bias contribution is no larger than the displayed stochastic term up to constants under the stated horizon condition. Dividing (35) by $nT\eta$ gives

$$\frac{1}{T} \sum_{k=0}^{T-1} \mathbb{E}[\|\nabla f(\bar{x}_k)\|^2] = \mathcal{O}\left(\sqrt{\frac{p}{nT}}\right) + \mathcal{O}\left(\frac{n}{T}\right). \quad (36)$$

Dividing the first term in (35) by T and using the same bound gives

$$\frac{1}{T} \sum_{k=0}^{T-1} \mathbb{E}\left[\frac{1}{n} \sum_{i=1}^n \|x_{i,k} - \bar{x}_k\|^2\right] = \mathcal{O}\left(\frac{n}{T}\right). \quad (37)$$

IX. APPENDIX D: DETAILED PROOF OF THEOREM 2

Under Assumption 5,

$$n \|\nabla f(\bar{x}_k)\|^2 \geq 2\nu n (f(\bar{x}_k) - f^*).$$

Substituting this into (8b) gives, for η_k small enough,

$$\mathbb{E}[W_{k+1}] \leq (1 - c\eta_k) \mathbb{E}[W_k] + C p \eta_k^2 + C p^2 \eta_k \delta_k^2. \quad (38)$$

The PL smoothing schedule satisfies $p^2 \eta_k \delta_k^2 \leq C p \eta_k^2$, hence

$$\mathbb{E}[W_{k+1}] \leq (1 - c\eta_k) \mathbb{E}[W_k] + C p \eta_k^2. \quad (39)$$

For $\eta_k = \kappa_\eta / (k + t_1)$ with $\kappa_\eta > 8/\nu$ and t_1 large enough, the standard Robbins–Siegmund sequence estimate applied to (39) gives

$$\mathbb{E}[W_T] = \mathcal{O}\left(\frac{p}{T}\right). \quad (40)$$

Because W_T is equivalent to $n(f(\bar{x}_T) - f^*) + \|\mathbf{x}_T\|_K^2/n$, this implies

$$\mathbb{E}[f(\bar{x}_T) - f^*] = \mathcal{O}\left(\frac{p}{nT}\right) + \mathcal{O}\left(\frac{p}{T^2}\right), \quad (41)$$

where the second term accounts for the residual disagreement contribution. Applying the disagreement recursion with the already established objective bound gives

$$\mathbb{E}\left[\frac{1}{n} \sum_{i=1}^n \|x_{i,T} - \bar{x}_T\|^2\right] = \mathcal{O}\left(\frac{p}{T^2}\right). \quad (42)$$

X. APPENDIX E: REPRODUCIBILITY DETAILS

For the black-box classification experiment, ZOOM-PB and ZOOM use the same coordinate estimator and the same communication graph; the only difference is $\gamma < 1$ versus $\gamma = 1$. For the UAV source-seeking experiment, the comparison curve in Fig. 3 uses the Gaussian-mixture field in the main text, a five-agent ring graph, the same two-point coordinate oracle for both methods, and identical primal consensus communication. Thus the observed gap in the concentration curve is attributable to the nonlinear gain rather than to a different query or communication budget.

REFERENCES

- [1] Z. Li, K. You, and S. Song, "Cooperative source seeking via networked multi-vehicle systems," *Automatica*, vol. 115, p. 108853, 2020.
- [2] J. C. Spall, *Introduction to stochastic search and optimization: estimation, simulation, and control*. John Wiley & Sons, 2005, vol. 65.
- [3] A. R. Conn, K. Scheinberg, and L. N. Vicente, *Introduction to Derivative-Free Optimization*. MPS-SIAM Series on Optimization. SIAM Philadelphia, 2009.
- [4] C. Audet and W. Hare, *Derivative-Free and Blackbox Optimization*. Springer, 2017.
- [5] J. Larson, M. Menickelly, and S. M. Wild, "Derivative-free optimization methods," *Acta Numerica*, vol. 28, pp. 287–404, 2019.
- [6] S. Ghadimi and G. Lan, "Stochastic first-and zeroth-order methods for nonconvex stochastic programming," *SIAM Journal on Optimization*, vol. 23, no. 4, pp. 2341–2368, 2013.
- [7] X. Lian, H. Zhang, C.-J. Hsieh, Y. Huang, and J. Liu, "A comprehensive linear speedup analysis for asynchronous stochastic parallel optimization from zeroth-order to first-order," in *Advances in Neural Information Processing Systems*, 2016, pp. 3054–3062.
- [8] Y. Nesterov and V. Spokoiny, "Random gradient-free minimization of convex functions," *Foundations of Computational Mathematics*, vol. 17, no. 2, pp. 527–566, 2017.
- [9] S. Liu, B. Kailkhura, P.-Y. Chen, P. Ting, S. Chang, and L. Amini, "Zeroth-order stochastic variance reduction for nonconvex optimization," in *Advances in Neural Information Processing Systems*, 2018, pp. 3727–3737.
- [10] D. Yuan and D. W. Ho, "Randomized gradient-free method for multiagent optimization over time-varying networks," *IEEE Transactions on Neural Networks and Learning Systems*, vol. 26, no. 6, pp. 1342–1347, 2014.
- [11] D. Yuan, S. Xu, and J. Lu, "Gradient-free method for distributed multiagent optimization via push-sum algorithms," *International Journal of Robust and Nonlinear Control*, vol. 25, no. 10, pp. 1569–1580, 2015.
- [12] Y. Tang, J. Zhang, and N. Li, "Distributed zero-order algorithms for nonconvex multiagent optimization," *IEEE Transactions on Control of Network Systems*, vol. 8, no. 1, pp. 269–281, 2020.
- [13] D. Hajinezhad, M. Hong, and A. Garcia, "ZONE: Zeroth-order non-convex multiagent optimization over networks," *IEEE Transactions on Automatic Control*, vol. 64, no. 10, pp. 3995–4010, 2019.
- [14] X. Yi, S. Zhang, T. Yang, and K. H. Johansson, "Zeroth-order algorithms for stochastic distributed nonconvex optimization," *Automatica*, vol. 142, p. 110353, 2022.
- [15] S. Zhang, Y. Dong, D. Xie, L. Yao, C. P. Bailey, and S. Fu, "Convergence analysis of nonconvex distributed stochastic zeroth-order coordinate method," in *IEEE Conference on Decision and Control*, 2021.
- [16] Y. Tang, Z. Ren, and N. Li, "Zeroth-order feedback optimization for cooperative multi-agent systems," *Automatica*, vol. 148, p. 110741, 2023.
- [17] Y. Yuan, M. Li, J. Liu, and C. Tomlin, "On the powerball method: Variants of descent methods for accelerated optimization," *IEEE Control Systems Letters*, vol. 3, no. 3, pp. 601–606, 2019.
- [18] S. Zhang and C. P. Bailey, "Accelerated zeroth-order algorithm for stochastic distributed non-convex optimization," in *2022 American Control Conference (ACC)*. IEEE, 2022, pp. 4274–4279.